

J. Matoušek  
On behalf of the COMPASS collaboration

# Quarkonium studies at COMPASS experiment

Received: *date* / Accepted: *date*

**Abstract** COMPASS is a fixed-target experiment with wide scientific programme. The main objectives are nucleon structure studies and hadron spectroscopy. A short overview of the physics programme and the apparatus is given. Then, three measurements that have a relation to quarkonium are highlighted and briefly described: a determination of limits on the exotic resonance  $Z_c^\pm(3900)$  branching ratio and partial width; study of the gluon Sivvers asymmetry in leptonproduction of  $J/\psi$  resonance and finally the first-ever study of the Drell–Yan process with a transversely polarised target.

**Keywords** COMPASS · fixed-target · nucleon structure ·  $J/\psi$  ·  $Z_c$  · gluon Sivvers asymmetry · Drell–Yan

## 1 Introduction

COMPASS [1] is a fixed-target experiment at CERN, which started physics data taking in 2002 and in 2012 entered its second phase with new scientific goals [2]. From the start COMPASS was designed as a multi-purpose apparatus. The main points of interest are nucleon structure studies, hadron spectroscopy and studies of chiral dynamics. Here we focus on the first; from the rest let us just name extensive studies of light meson spectrum (e.g. [3]) and measurements of  $\pi$  polarisability by scattering in the nuclear Coulomb field [4].

The spin structure of nucleons was studied in the COMPASS-I phase (2002–2011) in deep inelastic scattering (DIS) and semi-inclusive DIS (SIDIS) processes on longitudinally polarised targets  $\mu^+ + N^{\leftarrow} \rightarrow \mu^+ + X (+h)$  focusing on helicity distributions of quarks [5] and gluons [6–8] and in SIDIS on transversely polarised targets  $\mu^+ + N^{\uparrow} \rightarrow \mu^+ + X + h$  to investigate the transverse spin and transverse momentum structure of the nucleon [9–11].

In the COMPASS-II phase the knowledge of the nucleon structure is to be deepened further. In 2015 COMPASS collected data on Drell–Yan reaction with transversely polarised target  $\pi^+ + p^{\uparrow} \rightarrow \mu^+ + \mu^- + X$ , which (combined with the earlier SIDIS measurements) provides an important QCD universality test. A different way to the understanding of the nucleon structure leads via exclusive reactions like deep virtual Compton scattering (DVCS)  $\mu + p \rightarrow \mu + p + \gamma$ , which is being studied at COMPASS in 2016 and 2017.

COMPASS is not directly aimed at quarkonium studies, but thanks to its versatility it could bring interesting insights to the field. In the following the apparatus and several measurements, which have a link to the conference topics, are briefly described.

---

Presented at the workshop “New observables in quarkonium production”, Trento, Italy, 28. 2. – 4. 3. 2016.

Charles university in Prague and Trieste Section of INFN, [jan.matousek@cern.ch](mailto:jan.matousek@cern.ch)

## 2 Apparatus

Because of its challenging and wide physics focus, COMPASS was designed to offer large angular and momentum acceptance, including tracking from extremely small polar angles up to 180 mrad and particle identification [12, 13]. It makes use of a secondary beam of hadrons (mainly  $\pi$  or p) with energy up to 280 GeV/ $c$ , or a tertiary  $\mu$  beam with energy up to 190 GeV/ $c$ . The hadron beam is produced by the SPS proton beam hitting a beryllium target and sent to the experimental hall. Two differential Cherenkov counters are used for hadron beam particle identification. The  $\mu$  beam comes from decaying pions, which makes it naturally longitudinally polarised, and can have intensity up to about  $10^8$  s $^{-1}$ .

Arrangement of the target region differs for the various programmes. A large solid-state polarised target [12, 14] is used for SIDIS and Drell–Yan measurements. The target can be polarised in either longitudinal or transverse direction. A long liquid-hydrogen target together with a recoil proton detector installed around it or solid state nuclear targets are used as well [13].

To ensure the wide kinematic range, COMPASS spectrometer is divided in two stages each having its own dipole magnet, set of tracking detectors, electromagnetic and hadronic calorimeter and a muon filter. In addition, there is a Ring imaging Cherenkov counter for hadron identification in the first, large-angle stage. In both stages tracks with smaller polar angles are detected by conventional or pixelised micro-pattern gaseous detectors (GEMs and Micromegas), while at larger angles drift chambers, drift tube detectors and multi-wire proportional chambers are used.

## 3 Search for $Z_c^\pm(3900)$

The exotic  $Z_c^\pm(3900)$  state has been recently discovered by the BES-III and Belle collaborations in  $e^+ + e^- \rightarrow \pi^+ + \pi^- + J/\psi$  reactions at  $\sqrt{s} = 4.26$  GeV via the decay channel  $Z_c^\pm(3900) \rightarrow J/\psi + \pi^\pm$  [15, 16]. In the vector meson dominance (VMD) model it can be produced by the interaction of an incoming photon with a virtual charged pion coming from the target nucleon

$$\gamma + N \rightarrow Z_c^\pm(3900) + N. \quad (1)$$

At COMPASS the exclusive  $J/\psi$  production in photon-nucleon interaction

$$\mu^+ + N \rightarrow \mu^+ + J/\psi + N \rightarrow 2\mu^+ + \mu^- + N \quad (2)$$

has been observed in range  $\sqrt{s_{\gamma N}}$  from 7 to 19 GeV, as can be seen in Fig. 1 and 2a. A sizeable cross section for the reaction (1) with  $\sqrt{s_{\gamma N}} = 10$  GeV has been predicted [17]. All COMPASS muon data (2002–2011) have been analysed looking for the reaction

$$\mu^+ + N \rightarrow \mu^+ + Z_c^\pm(3900) + N \rightarrow \mu^+ + J/\psi + \pi^\pm + N \rightarrow 2\mu^+ + \mu^- + \pi^\pm + N. \quad (3)$$

The invariant mass spectrum of 970 events, which have been selected in total, does not exhibit any statistically significant resonant structure around 3.9 GeV/ $c^2$  (Fig. 2b). An upper limit for the number of produced  $Z_c^\pm(3900)$  events corresponding to confidence level of 90% has been determined to be 15.1 events [18].

Using the  $J/\psi$  production (2) for normalisation a limit on the branching ratio at  $\sqrt{s_{\gamma N}} = 13.8$  GeV

$$\text{BR}(Z_c^\pm(3900) \rightarrow J/\psi \pi^\pm) \times \frac{\sigma_{\gamma N \rightarrow Z_c^\pm(3900) N}}{\sigma_{\gamma N \rightarrow J/\psi N}} < 3.7 \times 10^{-3} \quad (4)$$

has been obtained [18]. Using  $\sigma_{\gamma N \rightarrow J/\psi N}$  measured by the NA14 collaboration and the VMD model finally an upper limit on the partial width of the decay  $Z_c^\pm(3900) \rightarrow J/\psi \pi^\pm$  as  $\Gamma_{J/\psi \pi} < 2.4$  MeV/ $c^2$  has been calculated, which can be compared with the total width measured by BES-III [15]  $\Gamma_{\text{tot}} = 46$  MeV/ $c^2$ . COMPASS thus has made a significant input to the discussion about the nature of the exotic state  $Z_c^\pm(3900)$  with the conclusion that if the assumptions of Ref. [17] are correct, the decay channel  $Z_c^\pm(3900) \rightarrow J/\psi \pi^\pm$  cannot be the dominant one [18].

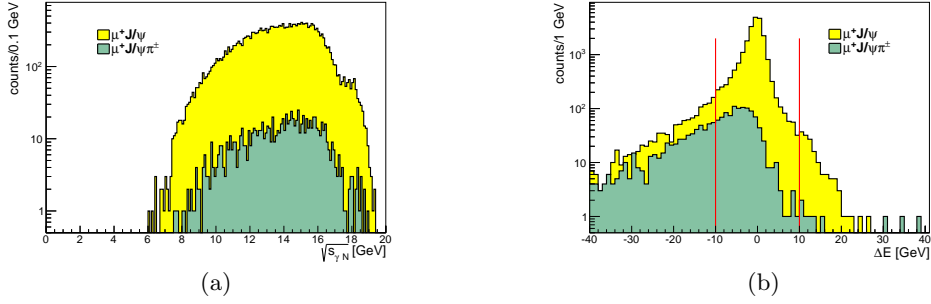


Fig. 1: Distributions of (a)  $\sqrt{s_{\gamma N}}$  and (b) energy balance  $\Delta E$  for reactions (2) (upper, yellow histogram) and (3) (lower, green histogram) [18]. The red lines represent cut on  $\Delta E$  used to select exclusive events.

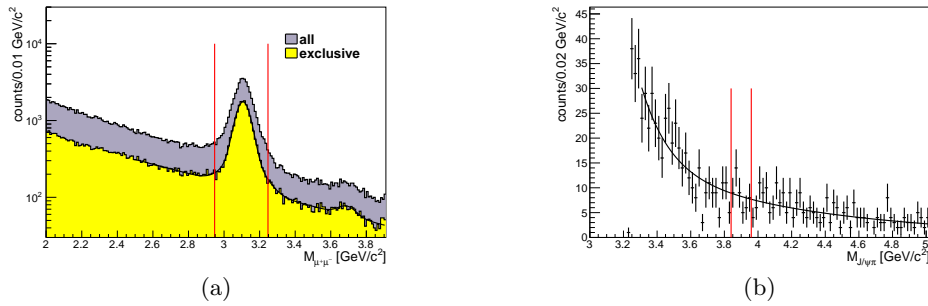


Fig. 2: (a) Invariant mass distribution for all dimuons produced in muon-nucleon scattering (upper, blue histogram), and for exclusively produced dimuons (lower, yellow histogram). The red lines represent cut used to select events compatible with  $J/\psi$  mass. (b) Invariant mass distribution of the  $J/\psi \pi^\pm$  state from the reaction (3). Fitted function used to describe the background is shown as a continuous black curve, the vertical red lines denote the signal region [18].

#### 4 Gluon Sivers function and $J/\psi$ leptonproduction

In the collinear picture, with parton transverse momentum component  $\mathbf{k}_T$  integrated over, the nucleon structure can be described by three parton distribution functions (PDFs): the number density, helicity and transversity, which depend on the fraction  $x$  of the nucleon momentum carried by the parton. Beyond this collinear approximation the description can be extended to include all possible correlations between parton spin, parton transverse momentum and parent nucleon spin. At leading twist the correlations are described in terms of 8 transverse-momentum dependent (TMD) PDFs, which depend apart from  $x$  also on the parton transverse momentum  $\mathbf{k}_T^2$ .

The Sivers TMD PDF [19] describes a correlation between parton transverse momentum and parent hadron transverse polarisation. Non-zero Sivers PDF of quarks gives rise to the Sivers asymmetry in SIDIS on transversely polarised nucleons. It has been measured to be different from zero for positive hadrons produced on protons by HERMES [20] and COMPASS [11]. An asymmetry of the same origin is expected in Drell–Yan reaction (Sec. 5).

Little is known experimentally about the gluon Sivers function [21, 22]. One of the possible ways of accessing it is a measurement of a Sivers-like asymmetry of hadrons, produced in the scattering of leptons off transversely polarised nucleons  $l + N^\uparrow \rightarrow l + h + X$  via the photon-gluon fusion (PGF) process  $\gamma + g \rightarrow q + \bar{q}$  [23]. When the  $q\bar{q}$  pair carries a heavy flavour, the other two single- $\gamma$  exchange processes (the leading process  $\gamma + q \rightarrow q$  and the QCD Compton process  $\gamma + q \rightarrow q + g$ ) are suppressed and the PGF dominates. This can be ensured in the production of the open-charm (beauty) [24, 25]

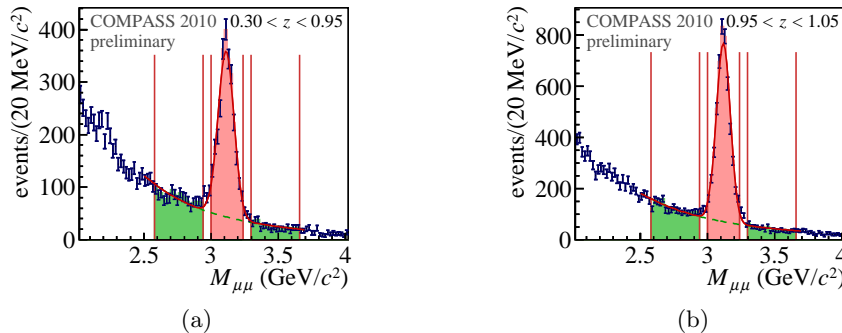


Fig. 3: The dimuon invariant mass distribution for the two  $z$  intervals. The signal region and side-bands are denoted. The red fit is the normal distribution plus a power-law background, which is in addition shown separately as the dashed green line [29].

or charmonium [26, 27]. The latter approach assumes that the  $q\bar{q}$ , which is produced by the PGF in the colour octet state, can transform into the colour singlet charmonium like in the colour evaporation model [28]. In the following, the preliminary COMPASS results for the charmonium (namely  $J/\psi$ ) production [29] are presented. Alternatively, the fact that the leading process is suppressed for high- $p_T$  hadron pairs can be utilised [30]. Preliminary results for the corresponding Siverts-like asymmetry have already been produced by COMPASS [31].

The  $J/\psi$  production  $\mu^+ + p^\uparrow \rightarrow \mu^+ + J/\psi + X$  has been studied in COMPASS data collected in 2010 with the 160 GeV/ $c$  muon beam and the transversely polarised proton ( $\text{NH}_3$ ) target. The  $J/\psi$  has been reconstructed from its decay into muons, so  $2\mu^+ + \mu^- + X$  have been looked for in the final state. Since the dominant mechanism of the  $J/\psi$  production can be different for the inclusive and exclusive cases, we have studied the reaction in two  $z$ -intervals [0.3, 0.95] and [0.95, 1.05], where  $z$  is the fraction of the available energy carried out by the  $J/\psi$

$$z \stackrel{\text{lab}}{=} \frac{E_{J/\psi}}{E_\mu - E_{\mu'}}. \quad (5)$$

A clear signal has been found in  $\mu^+\mu^-$  invariant mass spectra for both  $z$  intervals, as can be seen in Fig. 3. The spectra have been fitted with the normal distribution plus a power-law background. In the first  $z$  interval the peak position is  $M_{\mu\mu} = 3.110$  GeV/ $c^2$ , width  $\sigma = 59$  MeV/ $c^2$  and the signal over background ratio  $N_{\text{sig}}/N_{\text{bg}} = 4.31$ . In the second  $z$  interval the values are similar:  $M_{\mu\mu} = 3.12$  GeV/ $c^2$ , width  $\sigma = 52$  MeV/ $c^2$  and  $N_{\text{sig}}/N_{\text{bg}} = 5.25$ . The number of signal events has been found to be about 2300 and 4500 in the first and the second  $z$  interval respectively. The distribution of  $z$  is shown in Fig. 4a.

In the inclusive case ( $z < 0.95$ ), assuming the colour evaporation model, the gluon Siverts function should manifest itself in a  $\sin(\phi_h - \phi_S)$  modulation of the cross-section [26], where  $\phi_h$  is the azimuthal angle of the  $J/\psi$  momentum and  $\phi_S$  is the azimuthal angle of the target polarisation (in a reference frame where the  $z$ -axis is parallel to the  $\gamma^*$  momentum). The background asymmetry has been estimated from the side bands around the invariant mass peak and subtracted from the asymmetry of the signal.

The final asymmetry has been found to be compatible with zero [29], as can be seen in Fig. 4b. The limited statistics has resulted in a statistical uncertainty, which is large as compared with theoretical estimates for the asymmetry [26, 27]. An improvement could be done by utilising more optimised  $\mu$  reconstruction method and analysing COMPASS data from other transversely-polarised target runs; the estimated gain in statistics is about a factor of two.

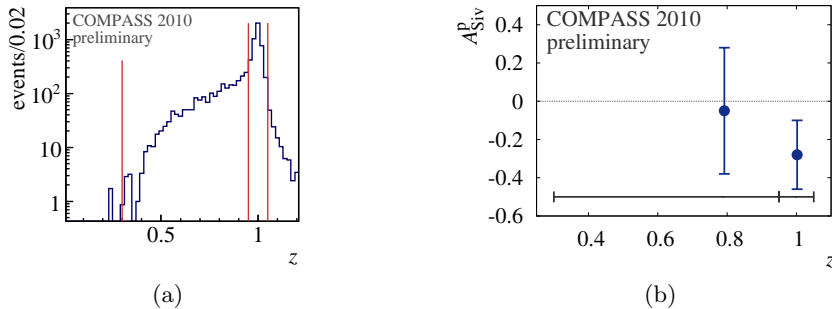


Fig. 4: (a) The distribution of  $z$  for all  $J/\psi$  events. The two intervals are denoted by red lines. (b) The Sivers-type asymmetry in  $J/\psi$  leptonproduction on proton target, the horizontal grey intervals denote integration ranges [29].

## 5 Drell–Yan programme

In its second phase COMPASS intends to complement the knowledge about the transverse-momentum dependent structure of nucleons by studying the Drell–Yan reaction with 190 GeV/c pion beam and transversely polarised proton target  $\pi^- + p^\uparrow \rightarrow \mu^+ + \mu^- + X$ . The cross section of this reaction [32] contains modulations proportional to convolutions of proton and pion TMD PDFs. This is at variance with SIDIS, where the TMD PDFs are convoluted with fragmentation functions [33]. The measurement of the polarised Drell–Yan reaction is an important test of the universality of the PDFs. In fact, two of the TMD PDFs – the Sivers and Boer–Mulders distributions – are not universal, but they are process-dependent in a defined way. Namely, it was shown that these two PDFs extracted from SIDIS and Drell–Yan reactions should have opposite signs [34]. Verification of the sign change of the u-quark Sivers PDF is the main motivation of the COMPASS Drell–Yan programme [2]. First experimental hints of the Sivers sign change have been recently given by the STAR experiment [35], but COMPASS has the opportunity to check the prediction directly, using SIDIS and Drell–Yan measurements in the same kinematic domain and taken on almost the same apparatus [36]. Another object of interest are the unpolarised part of the cross-section (Lam–Tung rule violation) and dimuon production on different nuclear targets (e.g. the EMC effect). The main attention is paid to the invariant mass range  $M_{\mu\mu} \in [4; 9]$  GeV/c<sup>2</sup>, where the TMD approach is expected to be valid ( $Q^2 = M_{\mu\mu}^2 \gg \mathbf{k}_T^2$ )<sup>1</sup> and, in addition, the background is extremely low. However, the region of the  $J/\psi$  and  $\psi'$  resonances is also considered interesting and will be analysed.

The Drell–Yan reaction has a relatively low counting rate, especially in the mass range above the  $J/\psi$  peak. Therefore, a beam with the highest available intensity (about  $10^8$   $\pi$ /s) has been used. COMPASS had never used such intense hadron beam before. A carefully designed hadron absorber with a tungsten beam plug has been placed right downstream of the polarised target to lower detector occupancies and radiation levels. The polarised target has been modified [14], a new large-area drift chamber for better large-angle tracking has been added and Micromegas detectors have been replaced by new ones with pixelised central parts to cope with higher particle flux. Finally the DAQ system has undergone a major upgrade to handle ageing of the original system and higher trigger rates [37]. A thin Al target has been used in parallel with the polarised NH<sub>3</sub> target and also the tungsten beam plug can be used as a nuclear target.

In 2014 a pilot run has been conducted with unpolarised target and with lower beam intensity. The modified spectrometer has been commissioned and data from about 10 days of stable operation have been collected. Preliminary analysis has shown that about 7 000 Drell–Yan events with invariant mass  $M_{\mu\mu} > 4$  GeV/c<sup>2</sup> are in the data. Distribution of the dimuon invariant mass and covered pion  $x$  – proton  $x$  region are shown in Fig. 5. As it is clear from Fig. 5b we probe the valence region where the

<sup>1</sup> This claim is supported by the dimuon transverse momentum distribution, which has been found to be peaked at about 1 GeV/c in the 2014 pilot run.

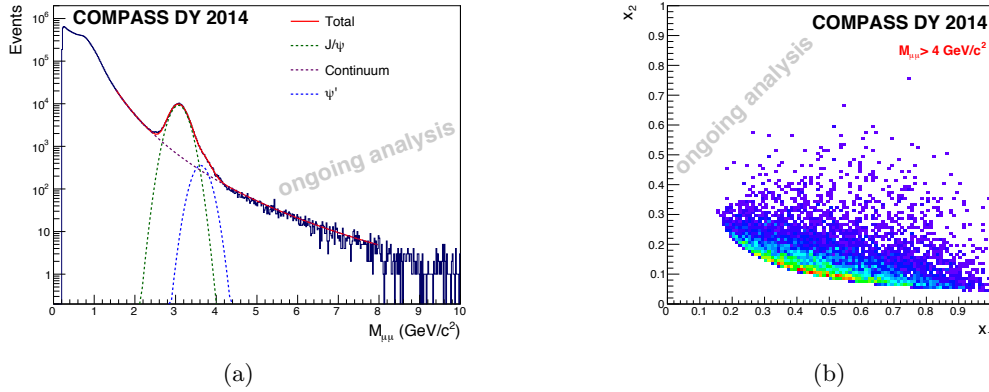


Fig. 5: (a) Dimuon invariant mass distribution from the pilot run after a preliminary set of cuts. The fit function is a power law plus two normal distributions representing the  $J/\psi$  and  $\psi'$  resonances. (b) Kinematic coverage in  $x_1$  (pion) and  $x_2$  (proton) for  $M_{\mu\mu} > 4 \text{ GeV}/c^2$ .

asymmetries are expected to be the strongest. The pilot run has confirmed the expected performance of the experiment.

The first-ever data on polarised Drell–Yan reaction have been collected by COMPASS in 2015 during a 140 days long run. The data are being analysed now. About 80 000 dimuons with  $M_{\mu\mu} > 4 \text{ GeV}/c^2$ , corresponding to an absolute statistical uncertainty of the Sivers asymmetry of about 2.8%, are expected. The first results from the year 2015 are expected soon and a possibility to have another 140 days of polarised Drell–Yan data taking in 2018 is under consideration.

## References

1. G. Baum, *et al.* [COMPASS Coll.], Tech. Rep. CERN-SPSLC-96-14, SPSLC-P-297 (1996). URL <http://cds.cern.ch/record/298433>.
2. F. Gautheron, *et al.* [COMPASS Coll.], Tech. Rep. CERN-SPSC-2010-014, SPSC-P-340 (2010). URL <http://cds.cern.ch/record/1265628>.
3. C. Adolph, *et al.* [COMPASS Coll.], Phys. Rev. Lett. **115**(8), 082001 (2015), [arXiv:1501.05732 \[hep-ex\]](https://arxiv.org/abs/1501.05732).
4. C. Adolph, *et al.* [COMPASS Coll.], Phys. Rev. Lett. **114**, 062002 (2015), [arXiv:1405.6377 \[hep-ex\]](https://arxiv.org/abs/1405.6377).
5. V.Yu. Alexakhin, *et al.* [COMPASS Coll.], Phys. Lett. **B647**, 8 (2007), [arXiv:hep-ex/0609038](https://arxiv.org/abs/hep-ex/0609038).
6. C. Adolph, *et al.* [COMPASS Coll.], Phys. Lett. **B718**, 922 (2013), [arXiv:1202.4064 \[hep-ex\]](https://arxiv.org/abs/1202.4064).
7. C. Adolph, *et al.* [COMPASS Coll.], Phys. Rev. **D87**(5), 052018 (2013), [arXiv:1211.6849 \[hep-ex\]](https://arxiv.org/abs/1211.6849).
8. C. Adolph, *et al.* [COMPASS Coll.], [arXiv:1512.05053 \[hep-ex\]](https://arxiv.org/abs/1512.05053) (2015). Submitted to Phys. Lett. B.
9. V.Yu. Alexakhin, *et al.* [COMPASS Coll.], Phys. Rev. Lett. **94**, 202002 (2005), [arXiv:hep-ex/0503002](https://arxiv.org/abs/hep-ex/0503002).
10. M. Alekseev, *et al.* [COMPASS Coll.], Phys. Lett. **B673**, 127 (2009), [arXiv:0802.2160 \[hep-ex\]](https://arxiv.org/abs/0802.2160).
11. C. Adolph, *et al.* [COMPASS Coll.], Phys. Lett. **B744**, 250 (2015), [arXiv:1408.4405 \[hep-ex\]](https://arxiv.org/abs/1408.4405).
12. P. Abbon, *et al.* [COMPASS Coll.], Nucl. Instrum. Meth. **A577**, 455 (2007), [arXiv:hep-ex/0703049](https://arxiv.org/abs/hep-ex/0703049).
13. P. Abbon, *et al.* [COMPASS Coll.], Nucl. Instrum. Meth. **A779**, 69 (2015), [arXiv:1410.1797 \[physics.ins-det\]](https://arxiv.org/abs/1410.1797).
14. J.H. Koivuniemi, *et al.*, PoS **PSTP2015**, 015 (2015).
15. M. Ablikim, *et al.* [BESIII Coll.], Phys. Rev. Lett. **110**, 252001 (2013), [arXiv:1303.5949 \[hep-ex\]](https://arxiv.org/abs/1303.5949).
16. Z.Q. Liu, *et al.* [Belle Coll.], Phys. Rev. Lett. **110**, 252002 (2013), [arXiv:1304.0121 \[hep-ex\]](https://arxiv.org/abs/1304.0121).
17. Q.Y. Lin, X. Liu, H.S. Xu, Phys. Rev. **D88**, 114009 (2013), [arXiv:1308.6345 \[hep-ph\]](https://arxiv.org/abs/1308.6345).
18. C. Adolph, *et al.* [COMPASS Coll.], Phys. Lett. **B742**, 330 (2015), [arXiv:1407.6186 \[hep-ex\]](https://arxiv.org/abs/1407.6186).
19. D.W. Sivers, Phys. Rev. **D41**, 83 (1990).
20. A. Airapetian, *et al.* [HERMES Coll.], Phys. Rev. Lett. **103**, 152002 (2009), [arXiv:0906.3918 \[hep-ex\]](https://arxiv.org/abs/0906.3918).
21. D. Boer, C. Lorcé, C. Pisano, J. Zhou, Adv. High Energy Phys. **2015**, 371396 (2015), [arXiv:1504.04332 \[hep-ph\]](https://arxiv.org/abs/1504.04332).
22. U. D'Alesio, F. Murgia, C. Pisano, JHEP **09**, 119 (2015), [arXiv:1506.03078 \[hep-ph\]](https://arxiv.org/abs/1506.03078).
23. D. Boer, P.J. Mulders, C. Pisano, J. Zhou, JHEP **08**, 001 (2016), [arXiv:1605.07934 \[hep-ph\]](https://arxiv.org/abs/1605.07934).
24. G. Altarelli, G.G. Ross, Phys. Lett. **B212**, 391 (1988).
25. M. Gluck, E. Reya, Z. Phys. **C39**, 569 (1988).
26. R.M. Godbole, A. Misra, A. Mukherjee, V.S. Rawoot, Phys. Rev. **D85**, 094013 (2012), [arXiv:1201.1066 \[hep-ph\]](https://arxiv.org/abs/1201.1066).

- 
27. R.M. Godbole, A. Misra, A. Mukherjee, V.S. Rawoot, Phys. Rev. **D88**(1), 014029 (2013), [arXiv:1304.2584 \[hep-ph\]](#).
  28. J.F. Amundson, O.J.P. Eboli, E.M. Gregores, F. Halzen, Phys. Lett. **B372**, 127 (1996), [arXiv:hep-ph/9512248 \[hep-ph\]](#).
  29. J. Matoušek [COMPASS Coll.], J. Phys. Conf. Ser. **678**(1), 012050 (2016).
  30. A. Bravar, D. von Harrach, A. Kotzinian, Phys. Lett. **B421**, 349 (1998), [arXiv:hep-ph/9710266](#).
  31. C. Adolph, *et al.*, (2017), [arXiv:1701.02453 \[hep-ex\]](#). Submitted to Phys. Lett. B.
  32. S. Arnold, A. Metz, M. Schlegel, Phys. Rev. **D79**, 034005 (2009), [arXiv:0809.2262 \[hep-ph\]](#).
  33. A. Bacchetta, M. Diehl, K. Goeke, A. Metz, P.J. Mulders, M. Schlegel, JHEP **02**, 093 (2007), [arXiv:hep-ph/0611265](#).
  34. J.C. Collins, Phys. Lett. **B536**, 43 (2002), [arXiv:hep-ph/0204004](#).
  35. L. Adamczyk, *et al.* [STAR Coll.], Phys. Rev. Lett. **116**(13), 132301 (2016), [arXiv:1511.06003 \[nucl-ex\]](#).
  36. C. Adolph, *et al.* [COMPASS Coll.], (2016), [arXiv:1609.07374 \[hep-ex\]](#). Accepted for publication in Phys. Lett. B.
  37. Y. Bai, M. Bodlak, V. Frolov, V. Jary, S. Huber, I. Konorov, D. Levit, J. Novy, D. Steffen, M. Virius, JINST **11**(02), C02025 (2016).